Particle Accelerators, 1991, Vol. 35, pp. 177–192
Reprints available directly from the publisher
Photocopying permitted by license only

DESIGN OF A SUPERCONDUCTING RFQ RESONATOR*

I. BEN-ZVI**, A. LOMBARDI§ and P. PAUL

Department of Physics, State University of New York at Stony Brook, NY, USA. 11794.

(Received 11 December 1991; in final form 26 October 1990)

We investigate the use of the Radio Frequency Quadrupole as a superconducting structure for heavy ion linacs. The concept, design and beam dynamics of the RFQlet, a short RFQ resonator, are described. The RFQlet combines the advantages of rf quadrupole focussing with the wide transit time factor curve, low stored energy, small size, and flexibility of the individual resonator approach, that is common to many modern booster linacs. The performance of the RFQlet may be optimized by using a universal curve relating to the ratio of accelerating field to peak-surface electric field to the basic RFQ geometry. This optimization leads to a procedure for the determination of all the RFQ parameters such as the modulation, aperture and voltage, resulting in a focusing factor B which decreases as a function of β and a constant accelerating field. We propose a novel "modulated phase focusing concept", whereby the stable phase is modulated between bunching and non-bunching. This technique increases the transverse stability of linacs without compromising the longitudinal acceptance. Finally, results of numerical simulation of the beam dynamics of an RFQlet positive ion injector are given.

1 INTRODUCTION

In a previous publication[1] we have described a design of a superconducting Radio Frequency Quadrupole (RFQ) injector that accelerates heavy ions from an ECR ion source with a velocity of $\beta = 0.01$ to about $\beta = 0.05$, the injection velocity of a typical heavy-ion superconducting linac.

A superconducting RFQ for heavy ions combines the superb charactersitics of the RFQ for slow ions with the cw operation and efficiency of superconducting linac structures.

The design considerations of a superconducting RFQ are quite different from those of a room temperature RFQ. On one hand we need not worry too much about the shunt resistance and high rf power considerations. On the other hand, problems like high mechanical stability, superconductor technology, size, and peak surface fields must be solved.

In this paper we present the novel concept of short, independently phased RFQ resonators (RFQlets), a design procedure for optimizing the acceleration of RFQs,

* This manuscript has been authored under grant number PHY-8902923 from the U.S. National Science Foundation.

** Also NSLS Department, Brookhaven National Laboratory, Upton NY 11973.
§ Permanent address LNL, Legnaro, Italy.

and an improved phasing scheme that enhances transverse stability for a given longitudinal acceptance. The use of these techniques should considerably improve the performance of RFQ linacs operating with low beam current, superconducting or otherwise. Relevant numerical examples will be presented to illustrate the applicability of these procedures to a heavy-ion injector at the velocity range of $\beta = 0.01$ to $\beta = 0.05$.

The use of short, independently powered resonators for the acceleration of heavy ions is standard technique in superconducting heavy-ion linacs. On the other hand, room-temperature RFQs have been long, multiple-$\beta\lambda$ structures. This is particularly true for high-current linacs, where one has to keep the beam under continuous focusing to counteract the strong divergence-creating forces of space charge.

The situation is different for a heavy-ion machine with low beam current. Here it is possible to subdivide the structure and introduce drift sections without incurring a penalty in terms of beam divergence. In fact, the transverse stability may even improve with this scheme, as we shall discuss later on. Furthermore, the low power consumption of a superconducting linac changes the economics of the machine to make such a scheme attractive. Obvious advantages of this method are:

1) A variable velocity profile;

2) Adjustable final energy;

3) Low stored energy per resonator;

4) Flexibility in the choice of resonator geometry as β changes;

5) Simplified construction and maintenance;

6) An additional degree of freedom in the beam dynamics due to the phasing of individual resonators;

7) Soft failure mode and–the loss of performance in a single resonator may be compensated in other resonators.

An obvious disadvantage is the increase in system complexity.

In any accelerating structure it is obviously important to maximize the accelerating gradient E_a. It has been observed[1,2] that by increasing the inter-electrode voltage V and bore radius a simultaneously along the RFQ linac ("tapering") one can improve the accelerating field in separate RFQ units[1] as well as in a single RFQ Here we present a quantitative optimization scheme of the RFQ parameters for this tapering procedure. For this purpose we derive a universal curve that relates E_a/E_s to RFQ parameters, i.e. the electrode minimum aperature a and the modulation factor m for a given particle velocity β and operating wavelength λ. The optimization which determines a, m and V, calls for a rapid tapering of the inter-electrodue voltage V. Such a tapering is greatly simplified by the use of RFQlets, where the voltage may be changed arbitrarily from one resonator to the next. In this scheme the accelerating field remains constant as β increases and the focusing strength B decreases.

Finally we discuss the beam dynamics of 'modulated phase focusing', a new method of enhancing the transverse focusing by alternating the stable phase angle between a bunching angle and 0 degrees (no bunching). The cells that have a synchronous

phase of 0 degrees (the crest of the accelerating field) produce a strong transverse focusing. These alternate with groups of cells where a strong bunching provides longitudinal stability. The modulated phase focusing method enables one to operate the RFQ stably with a small focusing parameter B (which otherwise would result in an instability) without compromising the longitudinal acceptance.

2 RFQlet RESONATOR DESIGN

In a superconducting resonator one of the most important parameters is the ratio of accelerating field E_a to the peak surface electric field E_s since electron field emission limits the operation of the superconducting resonator. On the other hand, a high average accelerating field is obviously desirable. Thus it is important to relate the resonator parameters to the ratio E_a/E_s and to maximize this ratio.

This ratio was shown[1] to be a function of m and ka:

$$E_a/E_s = \frac{kaA}{b\sqrt{\chi}},$$

where the acceleration parameter A is given by

$$A = \frac{m^2 - 1}{m^2 I_0(ka) + I_0(mka)}$$

and the focusing parameter χ is

$$\chi = 1 - AI_0(ka),$$

where I_0 is the modified Bessel function.

This ratio is valid for any modulation m and wave-number aperture product ka, (where $k = 2\pi/\beta\lambda$), as long as we use an electrode profile that generates a two-term potential.

The parameter b depends weakly on the transverse radius of curvature of the electrode and very weakly on m. A choice of $b = 5.8$ is a good approximation for the range of interest of these variables.

The optimum values of ka and E_a/E_s can then be obtained from the above expression. In order to facilitate design work, we present in Figure 1 a universal curve that approximately relates E_a/E_s to ka and m. In this curve we plot the normalized variable $\mathscr{R} = \nu(m)E_a/E_s$ as a function of $\mathscr{X} = \mu(m)ka$, where $\nu(m)$ and $\mu(m)$ are empirical functions:

$$\nu(m) = 5.7\,\frac{0.85m^2 + 2}{m^2 - 1}$$

and

$$\mu(m) = \frac{m + 1}{3 - 0.02m}.$$

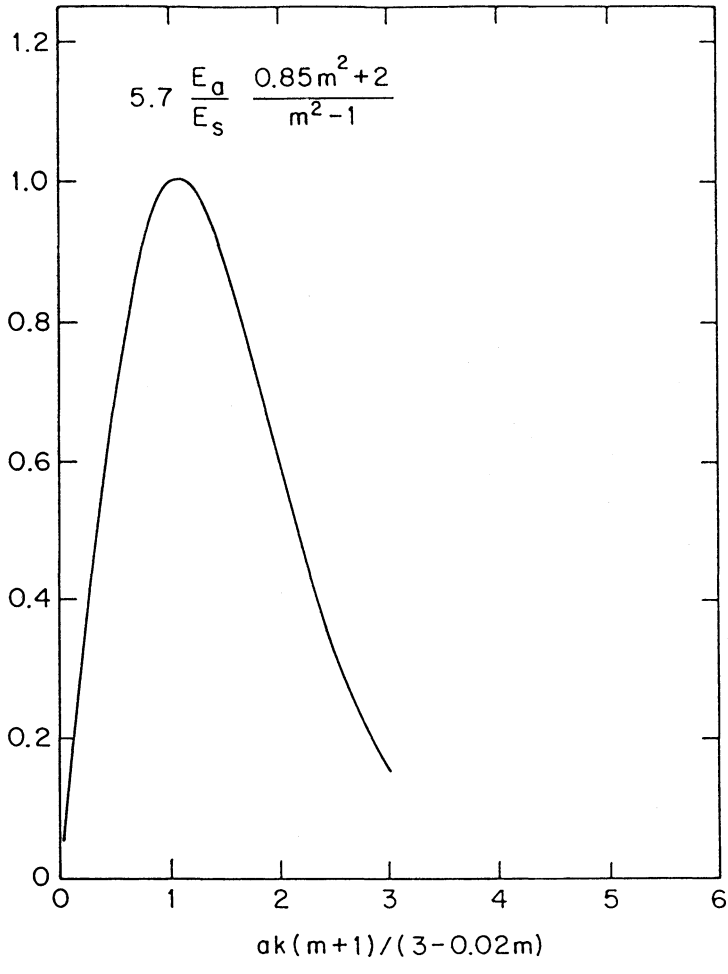

FIGURE 1 The universal curve relations the accelerating field to the peak surface electric field E_a/E_s in an RFQ with a two-term potential electrode shape. We plot $v(m)E_a/E_s$ vs. $\mu(m)ka$, where $v(m)$ and $\mu(m)$ are scaling functions.

The resulting curve has a maximum of $\mathscr{R} \approx 1$ at $\mathscr{X} \approx 1$. Thus the optimum value for ka is approximately

$$ka_{\text{opt}} \approx \frac{3}{m+1},$$

and the optimal field ratio is approximately

$$(E_a/E_s)_{\text{opt}} \approx \frac{m^2-1}{5.7(0.85m^2+2)}.$$

The universal curve in Figure 1 represents the ratio E_a/E_s with an accuracy better than $\pm 2.5\%$ for $2 \leq m \leq 6$ and $\mu(m)ka \leq 1$, which is the most useful range, being on the small-aperature side of the optimum. For $\mu(m)ka \leq 2$, the accuracy is better than $\pm 4\%$. The optimum values of ka and E_a/E_s given by the above simple relations are within $\pm 3\%$ of the exact values for $2 \leq m \leq 6$.

For very large modulations E_a/E_s tends to 1/4.8, which is an excellent ratio for heavy-ion linac structures. In practice one might limit m to moderate values of 4 or 5, which yield field ratios of 1:6 to 1:5.5, still very good values.

As suggested in[1] the optimal design of the superconducting RFQ uses an aperture a which changes along with β such as to keep ka constant at the optimal point, and to change the electrode voltage 'voltage tapering' in such a way as to keept E_s constant. This may be a difficult requirement, since k changes very dramatically in the low velocity range. However, the short, independently powered RFQ resonator makes this tapering easy.

How short can we make the RFQlet? In principle it is possible to design a true two-gap RFQlet which exhibits a very wide transit-time-factor curve[3]. In practice we have to compromise the width of the transit-time-factor curve against cost considerations and build 'multiple-gap' units. The exact optimum is not well defined and leaves a lot to personal choice.

The beam dynamics of an injector RFQ will be discussed in the next section. The optimal choice of ka in terms of the accelerating field results in a rather small focusing power B. Since the peak surface electric field and the charge-to-mass ratio of the ions to be accelerated are fixed by external design considerations (the nature of the superconducting surface and the ion source performance) the frequency is the only free parameter. The beam dynamics, through the focusing parameter B, thus determines the frequency. We choose a frequency of 50 MHz for the numerical calculation of the RFQ injector. This is the third subharmonic of the Stony Brook linac.

The size of a superconducting resonator is limited by consideration of manufacturing (surface preparations such as plating included) and the cryostat. The limited size and the relatively low inter-electrode capacitance (due to the large ratio of aperture a to electrode diameter) makes it necessary to adopt a lumped parameter resonator similar to the 'four-rod'[4] resonator. This choice of the resonant structure does not mean that the electrode shape has to be rodlike.

Figure 2 shows the conceptual design of such a resonator. The four electrodes are 'vane' shaped, with milled modulations $2\beta\lambda$ long. The electrodes are hollow to allow efficient liquid-helium cooling and to reduce weight. Each pair of electrodes is connected to a loop-like inductive electrode, which doubles as the cryogenic supply line. The loops are connected at their electrical centers by larger inductive electrodes to the top plate. Liquid helium is gravity-fed to the electrodes from a reservoir above the top plate. The whole assembly is surrounded by an upright cylindrical 'outer conductor' with beam ports and coupling holes built into it.

The frequency of this resonator can be estimated from simple lumped-circuit

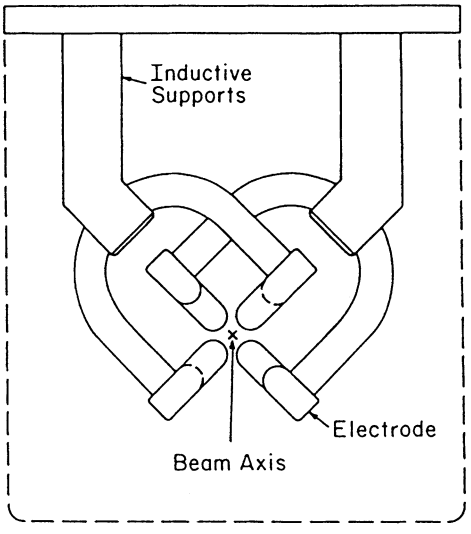

(a)

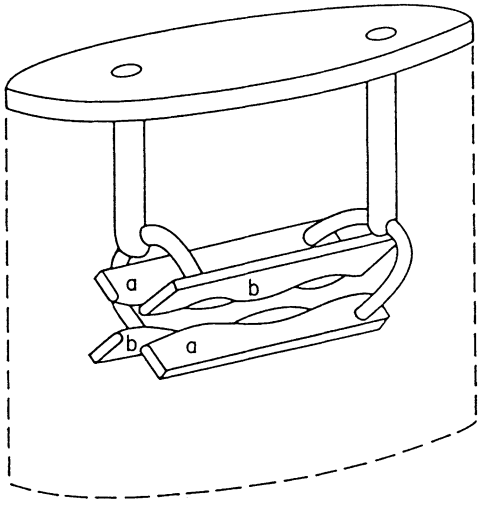

(b)

FIGURE 2 Schematic drawing of a two $\beta\lambda$ RFQ resonator. (a) Projection along the beam axis. The supports and electrodes are hollow (to be flooded with liquid helium). (b) General view. The electrodes marked 'a' are held at one potential and the 'b' electrodes are at a potential opposite to 'a'.

element equations. Total capacitance C can be written as[5] (units are rationalized MKS):

$$C/l_C \sim 10^{-12}\left(\frac{55.6}{\cosh^{-1}\left(\frac{r_0/\rho + 1}{\sqrt{2}}\right)} + \frac{21.21}{r_0/\rho - 0.414}\right),$$

where l_C is the total length of the RFQ rods, $r_0 = a/\sqrt{\chi}$ and ρ is the radius of the rods.

The two inductances leading from the rods to the top plate can be represented as a twin-conductor transmission line with impedance[6]:

$$Z = \frac{\eta}{\pi}\left[2p\frac{1-q^2}{1+q^2} - \frac{1+4p^2}{16p^2}(1-4q^2)\right],$$

where $\eta = 377\ \Omega$, $p = s/d$, $q = s/D$, d is the diameter of the conductors, s is their separation, and D is the diameter of the resonator's outer conductor. One has to include all the inductance from the top plate to the rods in the calculation. The main current splits into two equal currents that feed into the two vanes, which are at the same rf potential. Thus the above expression is an approximation where we assume an effective value for d and s.

The angular frequency ω of the resonator in terms of C and Z is the solution of

$$\tan\frac{\omega l_L}{c} = \frac{1}{Z\omega C},$$

which is the equation for a shorted transmission line of length l_L and characteristic impedance Z terminated at its open end by a capacitor C.

The stored energy is directly related to the capacitance:

$$U = \tfrac{1}{2}CV^2$$

The peak surface magnetic field in the resonator is determined by the capacitor charging current ωCV, which generates the field H on a conductor with diameter d:

$$H = \frac{\omega CV}{\pi d}.$$

The geometrical factor $\Gamma = QR_s$ is obtained by considering the loss generated by this current ωCV in the transmission line of length l_L:

$$\Gamma = \frac{\pi d}{2\omega C l_L}.$$

To put these expressions in perspective, let us take an RFQlet with $\beta = 0.03$ approximately (an intermediate value for our numerical example) and work out some numbers. We assume $r_0 = 3.4$ cm, $p = r_0/2$ and $l_C = 0.4$ m which results in $C = 21$ pF. For the inductive element we take $s = 0.19$ m, $D = 0.51$ m and $d = 0.073$ m. This yields a characteristic impedance of $Z = 468\ \Omega$. To get the frequency of 50 MHz takes a total conductor length of $l_L = 0.2$ m. If we further assume that the inter-

electrode voltage will be 0.42 MV, then the stored energy for this resonator will be 1.86 J, and the peak surface magnetic field 146 G. The geometrical factor turns out to be 87 Ω. These are reasonable values for superconducting resonators.

3 BEAM DYNAMICS OF RFQlets

The beam dynamics of an RFQ for its application as a heavy-ion superconducting injector has been described in a previous communication[1]. There are two new features in the present design, the use of short RFQ resonators and the scheme of modulated phase focusing. To introduce an intuitive feeling for the effect of these features on the beam optics we will initially use a transfer-matrix calculation in which β remains constant. Since this is a poor approximation for a working accelerator, we shall next use a numerical simulation of a practical RFQlet injector linac.

Subdividing the RFQ into independent resonators introduces drift spaces into the line structure. In order to study the effect of this on the transverse stability we consider the stable transverse transfer matrix P,

$$P = \begin{pmatrix} \cos\Omega + \alpha \sin\Omega & \beta^* \sin\Omega \\ \gamma \sin\Omega & \cos\Omega - \alpha \sin\Omega \end{pmatrix}.$$

In a $2\beta\lambda$ resonator, the transfer matrix is the product $P_1 = FDLFD$, where L is a drift matrix, D/F are single 'RFQ' cell defocusing/focusing matrices, and

$$F = \begin{pmatrix} \cos\Theta_+ & l_+ \sin\Theta_+ \\ -1/l_+ \sin\Theta_+ & \cos\Theta_+ \end{pmatrix}$$

$$D = \begin{pmatrix} \cosh\Theta_- & l_- \sinh\Theta_- \\ 1/l_- \sinh\Theta_- & \cosh\Theta_- \end{pmatrix},$$

where, as in[1], $\Theta_\pm^2 = \frac{1}{4}(B/\sqrt{2} \pm \Delta)$, $l_\pm^2 = 1/(B/\sqrt{2} \pm \Delta)$, and

$$\Delta = \frac{\pi^2}{2} \frac{qV}{Mc^2} \frac{A}{\beta^2} \sin\Phi.$$

Figure 3 shows the stability diagram B vs. Δ including the effect of the drift spaces. The three curves represent the boundaries of the stable region for no drift (upper curve), a drift of $\beta\lambda/2$ (center curve) and a drift of $\beta\lambda$ (bottom curve). We can see that the area of stability is actually extended to lower B values as the drift length is increased. This effect is to be expected since we are looking at the regime of low focusing strength in the RFQ, and thus, up to a limit, stability is enhanced by added drift spaces while keeping the lens strength constant. This effect disappears once space charge forces become significant.

Next we look at the effect of modulated phase focusing. Figure 4 shows the boundary of stability of the system represented by the transfer matrix P_2, where

$$P_2 = (F_0 D_0)^n (FD)^{2n} (F_0 D_0)^n$$

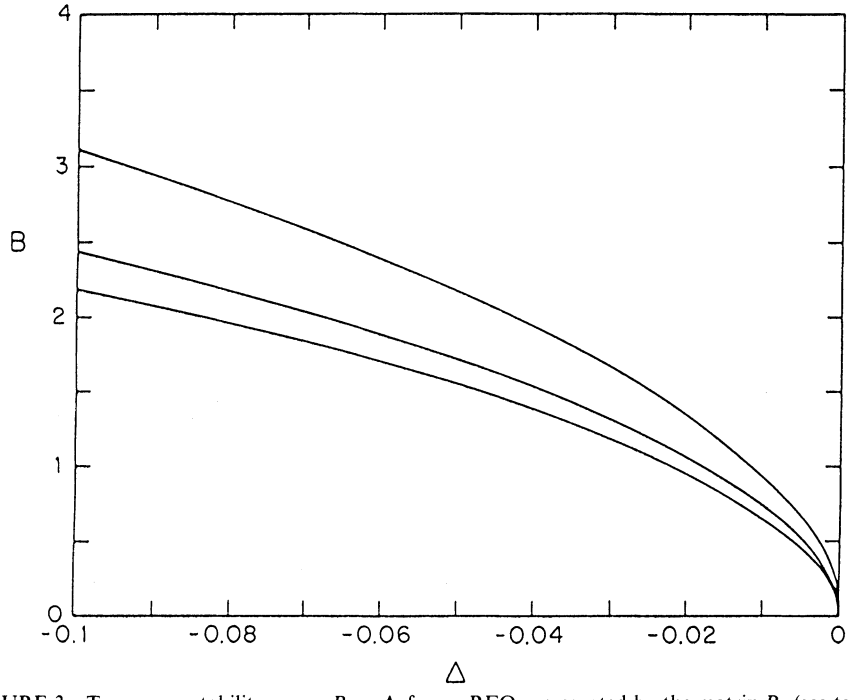

FIGURE 3 Transverse stability curve, B vs. Δ, for an RFQ represented by the matrix P_1 (see text). The stable areas lie above the respective curves. Top curve: no drift. Center curve: $\beta\lambda/2$ drift. Bottom curve: $\beta\lambda$ drift.

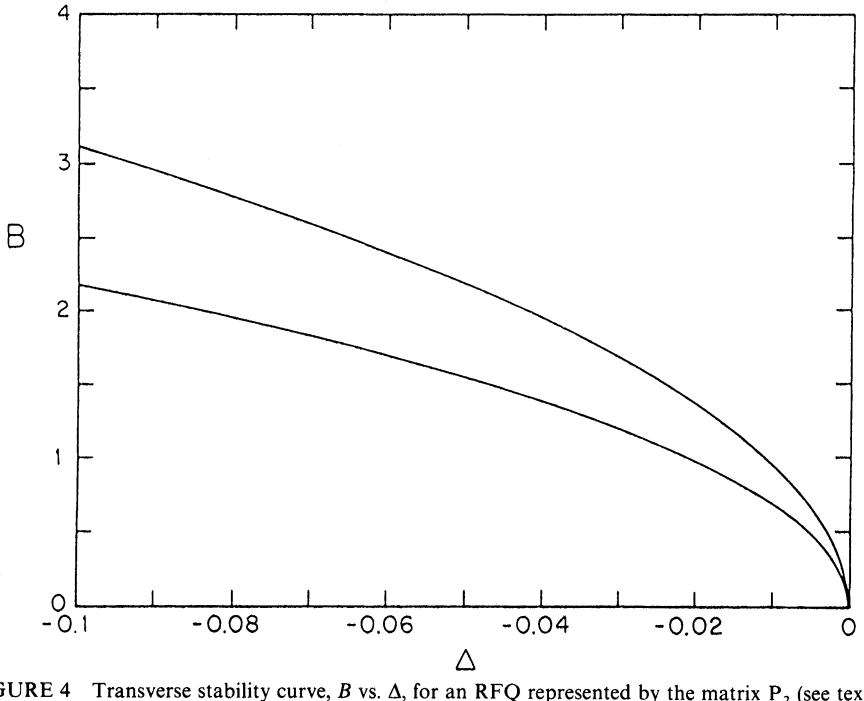

FIGURE 4 Transverse stability curve, B vs. Δ, for an RFQ represented by the matrix P_2 (see text). Top curve: conventional RFQ scheme. Bottom curve: modulated phase focusing.

and $2n$ is the number of RFQ cells which have the same stable phase; in the case of Figure 4 we took $n = 1$. The upper curve represents the case of conventional RFQ focusing, that is, $F_0 = F$ and $D_0 = D$. However in the modulated phase focusing case (lower curve) we calculate F_0 and D_0 with $\Delta = 0$, obtained by having $\sin \Phi_s = 0$.

Figure 4 shows clearly the advantage of the modulated phase focusing. The region of stability (which is above the relevant curve) moves to lower B values relative to the regular RFQ focusing scheme. This effect is more pronounced for n larger than 1 (not shown).

The interpretation of Figure 4 requires a correct choice of Δ, to be derived from considerations of the longitudinal motion. The longitudinal acceptance should be the same for both focusing schemes. The longitudinal acceptance is proportional to $E_a^{1/2}\Phi_s^{2.5}$ (where $\sin \Phi_s \approx \Phi_s$). E_a is the amplitude of the traveling wave component whose phase velocity is that of the synchronous particle. It can be shown that, when the phase is alternated rapidly between Φ_s and 0, the effective traveling wave will have a phase Φ_s but amplitude $\frac{1}{2}E_a$. Let us compare the modulated phase scheme with phase Φ_m to the constant phase scheme with phase Φ_s. The two schemes will have the same longitudinal acceptance if

$$(\tfrac{1}{2}E_a)^{1/2}(\Phi_m)^{5/2} = (E_a)^{1/2}(\Phi_s)^{5/2},$$

which results in

$$\Phi_m = 2^{1/5}\Phi_s.$$

A point (B, Δ) on the border of the stability curve for constant phase focusing should then be compared to a point (B_m, Δ_m) on the border of stability of the modulated phase focusing, where $\Delta_m \approx 1.15\Delta$. We observe that B_m will be smaller than B, indicating that the modulated phase focusing method results in stability with a smaller focusing parameter than does constant phase focusing.

If the phase is not alternating rapidly (the phase advance per section of constant Φ_s is large), numerical simulation may be done to show that to a good approximation the same relationship between Φ_m and Φ_s still holds.

The modulated phase focusing method is not limited to RFQ linacs. It differs from the well known alternating phase focusing[7] both in the choice of the synchronous phase and in the performance. In particular, alternating phase focusing results in a much smaller longitudinal acceptance.

The optimization of the accelerating field in the RFQ (Section 2) has implications for the beam dynamics. We had chosen a large modulation value m and a product ka which optimizes E_a/E_s according to the universal curve of Figure 1. At the same time we hold the surface field E_s constant. The focusing parameter B is given by

$$B = \frac{q}{Mc^2}\frac{V\sqrt{\chi}}{a}\lambda^2\sqrt{\chi}\frac{1}{a},$$

where the term q/Mc^2 is constant for a given beam, the term $V\sqrt{\chi}/a$ is constant for a constant surface field, and the term $\lambda^2\sqrt{\chi}$ is constant for a given frequency and for a constant value of ka. Thus B is inversely proportional to a, and from the constancy of ka it follows that B is inversely proportional to β. We note that the

optimization of the acceleration via the increase of m and a reduces the focusing strength B.

What is the trajectory of the operating point in the (B, Δ) plane as β increases? Δ is inversely proportional to β, since $A(ka)$ is constant and V is proportional to β. Thus the ratio B/Δ is constant. However the lower boundary of the stability region is given (to first order in Δ) by $B^2 = -8\pi^2\Delta$, so that care must be taken not to lose transverse stability with the increase in β.

Another effect of the decrease B as a function of β is an increase in the Courant–Snyder β^* function. However, this increase is partially compensated by the decrease in the geometrical emittance ε, $(\varepsilon = \varepsilon_n/\beta)$. Thus the beam envelope growth is very moderate as can be seen in the numerical simulation.

We have carried out a beam dynamics numerical simulation using the computer code PARMTEQ[8]. In this simulation we introduce drift spaces between individual RFQ resonators as well as modulated phase focusing. The RFQ linac parameters are based on our previous work[1], starting with lead ions from an ECR ion source and finishing with a beam that could be injected into the SUNY superconducting linac.

The main parameters for the beam dynamics numerical simulation are:

1) Input beam velocity $\beta = 0.01$;

2) Input beam lead 208 with a charge of 35;

3) Input normalized transverse emittance 0.1π mm mrad for both transverse planes;

4) Input phase spread 20 degrees total (1.1 ns);

5) Input energy spread 0.070 MeV total $(dW/W = 10^{-4})$;

6) Resonator frequency 50 MHz;

7) Peak surface electric field 16 MV/m.

We need six resonators to achieve $\beta = 0.05$. The ECR beam was matched into the accelerating structure using the α,β^* and γ functions obtained by evaluating the elements of the transfer matrix P given above.

The RFQ parameters were set using the following principles:

The length of the resonators was held to between 38 cm and 58 cm. The first and second resonators have a large number of cells due to the low value of β there. The next four have four cells each. A large value of the modulation constant m was chosen in order to get a large accelerating field. This value is 4 in the last four resonators, but slightly smaller, 3.5, in the first two resonators where we have a good accelerating field and thus may use a lower modulation and thereby enhance the transverse focusing. We do not use the modulated phase focusing in the first two resonators to avoid having two different values of the stable phase in a single resonator.

The functional dependence of $v(m)$ is such that increasing m brings a diminishing return in acceleration, while the geometry of the resonator becomes increasingly difficult. The choice of $m = 4$ is somewhat arbitrary.

Once we have m, we select ka using the universal curve for optimizing the acceleration. Since k is determined by the beam velocity, we obtain an a value which

TABLE 1
RFQ resonator and beam parameters for a superconducting positive ion injector simulation problem.

Resonator	1	2	3	4	5	6
Length (m)	0.37	0.42	0.42	0.46	0.52	0.58
Cells	12	8	4	4	4	4
β_{in}	0.0100	0.0210	0.0303	0.0358	0.0408	0.0463
β_{out}	0.0210	0.0303	0.0358	0.0408	0.0463	0.0514
V (MV)	0.135	0.285	0.419	0.464	0.535	0.607
a_{in} (cm)	0.670	1.1	1.57	1.68	1.94	2.2
a_{out} (cm)	0.699	1.316	1.57	1.68	1.94	2.2
m	3.5	3.5	4	4	4	4
A_{in}	0.662	0.733	0.758	0.781	0.778	0.778
A_{out}	0.802	0.768	0.794	0.804	0.801	0.798
B_{in}	4.9	3.2	2.0	1.83	1.59	1.41
B_{out}	3.1	2.0	1.8	1.68	1.47	1.32
$E_a(MV/m)$	1.8	2.2	2.6	2.5	2.5	2.6
Φ_s (Deg)	−15	−15	0	−25	0	−25
E_{in} (MeV)	9.7	42.71	88.72	124.6	161.5	208.0
E_{out} (MeV)	42.71	88.72	124.6	161.5	208.0	256.0

changes with β. Actually, we did not take ka values which correspond to the exact maximum of the E_a/E_s curve, but ones slightly on the low ka side of it. This choice enhances the transverse focusing without a significant sacrifice in acceleration. For example, in the first resonator we choose ka to be 7% below optimum. This results in acceleration only 1.5% smaller, but the β^* is smaller by nearly a factor of 2.

As the beam moves from one resonator to the next, β increases and the optimal a becomes larger. However, we increase the voltage V in order to keep the surface electric field constant.

The tapering of a and V is achieved by stepping their values from one resonator to the next. However within resonators 1 and 2, a is tapered slightly in order to provide continuity of the focusing parameter B in the transition between resonators.

The stable phase Φ_s, used in resonators 3 through 6 is chosen conservatively. The resulting separatrix is much larger than the beam's longitudinal emittance.

The resonator and beam parameters are listed in Table 1.

The acceleration gradient E_a includes the transit time factor. The lengths shown in Table 1 do not include the drift spaces. The simulation has 20 cm drift spaces between resonators. This drift represents the net distance from the electrodes of one resonator to the electrodes of the next. The effect of fringe fields has not been included.

TABLE 2
Comparison of transverse emittance growth for three phasing schemes.

Case	$\frac{\varepsilon^x_{out}}{\varepsilon^x_{in}}$	$\frac{\varepsilon^y_{out}}{\varepsilon^y_{in}}$	x_{out} (mm)	y_{out} (mm)
1	1.16	1.20	3.2	3.8
2	1.20	1.24	4.6	4.2
3	1.40	1.56	12.7	6.2

The resulting acceleration parameter A is a large and nearly constant, while the focusing parameter B is relatively small and decreasing with β. Since we are injecting a pre-bunched and chopped beam with a good emittance, there is no particle loss in the PARMTEQ simulation (the transmission efficiency is 100%). Furthermore, we observe a good linearity of the acceleration process. The increase in the transverse normalized emittance is very small (see Table 2 case 1). We observe a longitudinal emittance growth $\varepsilon_{out}/\varepsilon_{in} = 1.77$ which is due in part to coupling between the transverse and longitudinal motions.

What is the contribution of the modulated phase focusing, and how does it compare to the conventional scheme in the numerical simulation done with PARMTEQ? For this purpose we present a comparison of three simulations in which the only change was in the phases of resonators 3 through 6. The results are presented in Table 2. Case 1 is the modulated phase focusing given in Table 1, with Φ_s of resonators 3 to 6 alternating between 0 and -25 degrees. Case 2 is regular focusing, with Φ_s taken as -12.5 degrees in these resonators. As discussed above, this choice will result in a smaller longitudinal acceptance than case 1; however, since the longitudinal emittance in this simulation is very small, no particles are lost. Case 3 is also conventional focusing; however, with $\Phi_s = -21.7$ degrees. This is the proper comparison to Case 1, having the same longitudinal acceptance. $\varepsilon^x_{out}/\varepsilon^x_{in}$, $\varepsilon^y_{out}/\varepsilon^y_{in}$ is the relative normalized emittance growth in x, y along the linac. x_{out}, y_{out} is half the beam envelope in x, y. It is clear that the modulated phase focusing (Case 1) results in better transverse beam dynamics than the conventional focusing (Cases 2 and 3). The

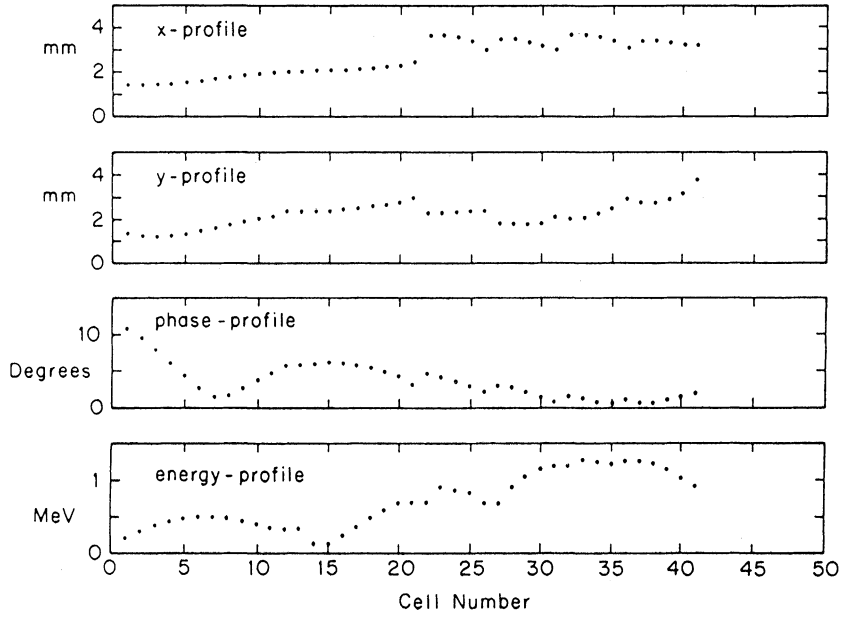

FIGURE 5 PARMTEQ particle dynamics results for: beam envelopes as a function of the cell number (see the text for the simulation parameters). a) x profile, b) y profile, c) phase profile and d) energy profile.

contrast is striking when the cases with equivalent longitudinal acceptance are compared (Cases 1 and 3).

The beam envelopes in x, y, phase and energy as computed by PARMTEQ are given in Figure 5. The envelopes are displayed as a function of the cell number. To relate the cell number to position in the injector linac, refer to Table 1.

The distribution of the beam particles in phase space is given in Figure 6 for the input and in Figure 7 for the end of the linac. There is no visible distortion of the particle distribution, as expected from the rather minimal increase of the normalized emittance.

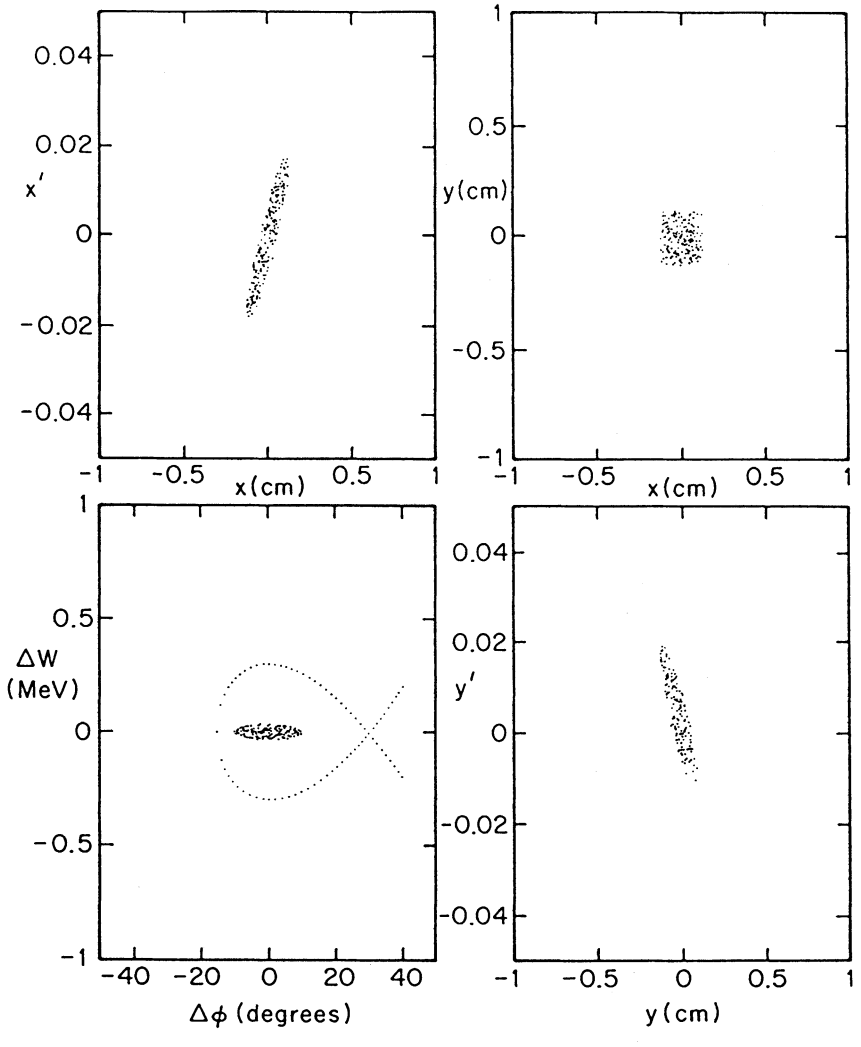

FIGURE 6 Input phase space diagrams for the PARMTEQ simulation. The dotted curve shown in the longitudinal phase space diagram is the separatrix at the input of the first RFQ resonator.

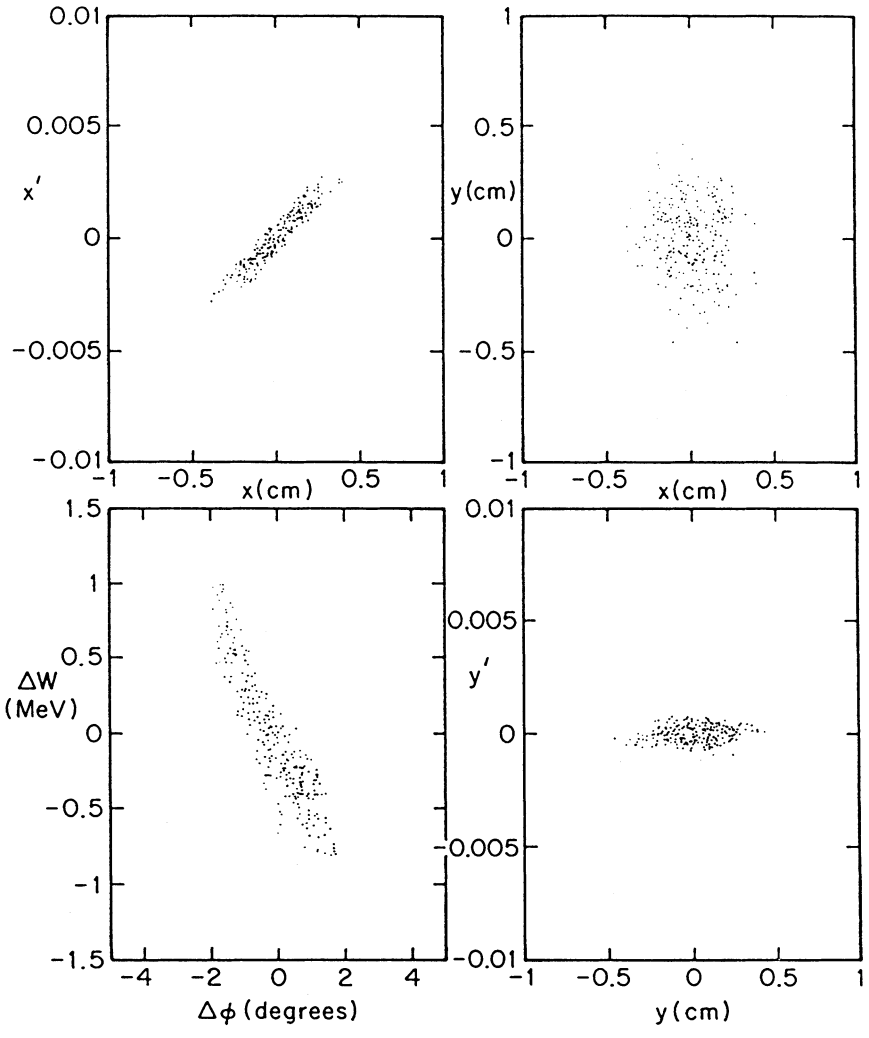

FIGURE 7 Phase space diagrams at the end of the simulated RFQ linac. The separatrix is too large to show in the longitudinal phase space diagram.

Finally, in order to demonstrate one of the advantages of the RFQlet concept, we have simulated a severe loss of performance, 40% of the nominal voltage, in resonator number 4. This loss is then compensated by an increase of 20% in the voltage of the two adjacent resonators, numbers 3 and 5, without a change in phasing.

As a result the output energy has changed slightly, from 256 MeV to 252 MeV. The beam remained stable, and the emittances did not change appreciably, being $\epsilon_{out}/\epsilon_{in} = 1.16$ for both transverse planes and 1.82 for the longitudinal phase space.

4 SUMMARY

The concept, design and beam dynamics of a short RFQ resonator (RFQlet) have been described. The RFQlet combines the advantages of rf quadrupole focusing with the wide transit-time-factor curve, low stored energy and small size of the independently powered resonator. Thus the RFQlet may make a very good superconducting resonator.

Furthermore we show how to use: 1) a universal curve relating the accelerating to peak surface electric fields ratio to the basic RFQ geometry and 2) a correlated tapering (increase) of voltage and aperture resonator by resonator to increase significantly the energy gain of the RFQ linac.

We introduce 'modulated phase focusing' whereby the stable phase is modulated between bunching and non-bunching and find that it enhances transverse stability without a penalty in longitudinal acceptance. This method can be used in any linac.

A numerical simulation of the beam dynamics of an RFQ positive ion injector was described and the parameter choice for the simulation has been explained in light of the accelerating field optimization, tapering procedure, and modulated phase focusing scheme.

An RFQlet is currently under construction at the State University of New York at Stony Brook. The resonator parameters are those of resonator number 3 in Table 1. The conductor technology being used is lead-tin plated on copper. Problems under study are frequency stability, multi-pactoring barriers and high-field performance as well as high-order terms in the Fourier-Bessel expansion of the potential function under the conditions of a large modulation factor and small transverse radius of curvature.

REFERENCES

1. I. Ben-Zvi, Part. Accel. **23**, 265 (1988).
2. B. G. Chidley, G. E. McMichael and R. M. Hutcheon, in *Proceedings of the 1987 Particle Accelerator Conference*, IEEE Trans. Nucl. Sci. **87CH2387-9**, 1913, (1987).
3. I. Ben-Zvi, Nucl. Instr. and Meth. A**287**, 306 (1990).
4. A. Schempp, M. Ferch and H. Klein, 1987 Particle Accelerator Conference, IEEE Trans. Nucl. Sci. **87CH2387-9**, 267, (1987).
5. R. M. Hutcheon (private communication).
6. S. Ramo, J. R. Whinnery and T. Van Duzer, *Fields and Waves in Communication Electronics* (John Wiley and Sons, Inc., New York, 1967, 444.
7. M. L. Good, *Phys. Rev.*, **92**, A538 (1953).
8. K. R. Crandall, R. H. Stokes, and T. P. Wangler, *in Proceedings of the 1979 Linac Conference*, Montauk, LA-UR 79-2499, 205. N.Y., (1979).